NEURAL REGENERATION RESEARCH
Volume 7, Issue 26, September 2012
www.nrronline.org

doi:10.3969/j.issn.1673-5374.2012.26.006 [http://www.crter.org/nrr-2012-qkquanwen.html]
Li ZY, Xia X, Rong XM, Tang YM, Xu DC. Structure of the brachial plexus root and adjacent regions displayed by ultrasound imaging. Neural Regen Res. 2012;7(26):2044-2050.

Structure of the brachial plexus root and adjacent regions displayed by ultrasound imaging**☆

Zhengyi Li[1, 2], Xun Xia[1], Xiaoming Rong[3], Yamei Tang[3], Dachuan Xu[1]

1 *Institute of Clinical Anatomy, Southern Medical University, Guangzhou 510515, Guangdong Province, China*
2 *Department of Ultrasound, Shenzhen Second People's Hospital, Shenzhen 518035, Guangdong Province, China*
3 *Department of Neurology, Sun Yat-sen Memorial Hospital, Sun Yat-sen University, Guangzhou 510120, Guangdong Province, China*

Abstract

Brachial plexuses of 110 healthy volunteers were examined using high resolution color Doppler ultrasound. Ultrasonic characteristics and anatomic variation in the intervertebral foramen, interscalene, supraclavicular and infraclavicular, as well as the axillary brachial plexus were investigated. Results confirmed that the normal brachial plexus on cross section exhibited round or elliptic hypoechoic texture. Longitudinal section imaging showed many parallel linear hypo-moderate echoes, with hypo-echo. The transverse processes of the seventh cervical vertebra, the scalene space, the subclavian artery and the deep cervical artery are important markers in an examination. The display rates for the interscalene, and supraclavicular and axillary brachial plexuses were 100% each, while that for the infraclavicular brachial plexus was 97%. The region where the normal brachial plexus root traversed the intervertebral foramen exhibited a regular hypo-echo. The display rate for the C_{5-7} nerve roots was 100%, while those for C_8 and T_1 were 83% and 68%, respectively. A total of 20 of the 110 subjects underwent cervical CT scan. High-frequency ultrasound can clearly display the outline of the transverse processes of the vertebrae, which were consistent with CT results. These results indicate that high-frequency ultrasound provides a new method for observing the morphology of the brachial plexus. The C_7 vertebra is a marker for identifying the position of brachial plexus nerve roots.

Key Words

brachial plexus; ultrasound; anatomical characteristics; CT; nerve root; brachial plexus block; neural regeneration

Research Highlights

(1) Using ultrasound imaging, the distribution of the brachial plexus and adjacent regions was investigated from the region where the brachial plexus root traverses the intervertebral foramen to the axillary fossa.
(2) Ultrasound demonstrated that the C_7 vertebra was the best localization marker to identify the nerve root.

Zhengyi Li☆, M.D., Associate chief physician, Institute of Clinical Anatomy, Southern Medical University, Guangzhou 510515, Guangdong Province, China; Department of Ultrasound, Shenzhen Second People's Hospital, Shenzhen 518035, Guangdong Province, China

Corresponding author: Dachuan Xu, Professor, Doctoral supervisor, Institute of Clinical Anatomy, Southern Medical University, Guangzhou 510515, Guangdong Province, China; Yamei Tang, M.D., Associate professor, Master's supervisor, Department of Neurology, Sun Yat-sen Memorial Hospital, Sun Yat-sen University, Guangzhou 510120, Guangdong Province, China chjcana@126.com; yameitang@hotmail.com

Received: 2012-05-11
Accepted: 2012-07-10
(N20120107003/WLM)

INTRODUCTION

Brachial plexus block has been extensively used in upper limb surgery. The block depends on the accuracy of localization. The localization of the brachial plexus depends on anatomical markers on the body surface. Because there is no objective index, puncture is repeated to locate sites of abnormal sensation, which often results in postoperative complications. Moreover, for patients who cannot cooperate or express abnormal sensation, the procedure is more

difficult, which frequently results in incomplete brachial plexus block. A nervestimulator can elevate the success rate of brachial plexus block, but it has disadvantages; it is time-consuming, and there is the risk of incomplete block or complications[1-3]. With the development of diagnostic ultrasound equipment and diagnostic techniques, clinicians chiefly focus on superficial soft tissue visualized by ultrasound[4-5]. Previous studies have shown that high-frequency ultrasound can be used successfully for brachial plexus block, but there are only a few descriptions of the morphology of the brachial plexus. In particular, there is no study on the brachial plexus root of the intervertebral foramen[6-7].

In the present study, we investigated the utility of ultrasound as an examination method for the normal brachial plexus and its anatomical characteristics. This was performed to further our understanding of the anatomical relationship between the brachial plexus and surrounding tissues and its significance in clinical application. Specifically, we investigated the morphology and distribution of the brachial plexus using ultrasonograms of different regions using high-frequency color Doppler ultrasound, and compared this with CT scan results.

RESULTS

Quantitative analysis of subjects

110 healthy subjects were included in the final analysis.

Ultrasonic imaging of the brachial plexus

Ultrasonograms of the brachial plexus long-axis displayed multiple hypo-echoes. Short-axis view displayed multiple round or elliptic hypo-echoes. Punctate high echo was visible in the internal part, which was surrounded by membrane-shaped echoes, with the presence of a clear boundary. Sonographic appearance was different on different observation planes (Figure 1).

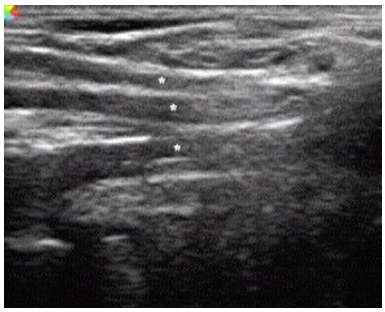

Figure 1 High-frequency color Doppler ultrasonography of the brachial plexus long-axis displayed multiple hypo-echoes (asterisks).

High-frequency ultrasound clearly displayed the bony outline of the anterior and posterior tubercles of the transverse processes of the vertebrae. The inner diameter and morphology of the bony outline at the nerve root exit zone were consistent with that measured by CT (Table 1). High-frequency ultrasound clearly displayed the outline of the transverse process of the vertebra (Figures 2, 3).

Table 1 The distance between (mm) anterior and posterior tubercles of the transverse process of the C_{5-7} vertebra of healthy adults measured by CT *versus* ultrasound

Method	C_5	C_6	C_7
CT	4.21±0.23	4.22±0.24	Absence of anterior tubercle
Ultrasound	4.14±0.26	4.13±0.27	Absence of anterior tubercle

The data are expressed as mean ± SD, n = 20. One-way analysis of variance revealed no significant difference between CT and ultrasound measurements (P > 0.05).

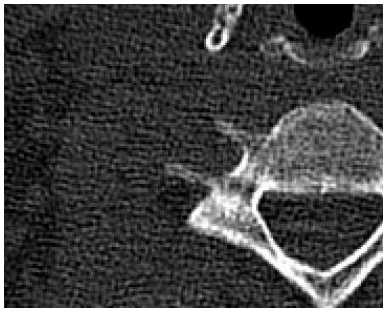

Figure 2 High-frequency color Doppler ultrasound exhibiting bony outline of anterior and posterior tubercles of the transverse process of the vertebra where the brachial plexus root originates in healthy adults.

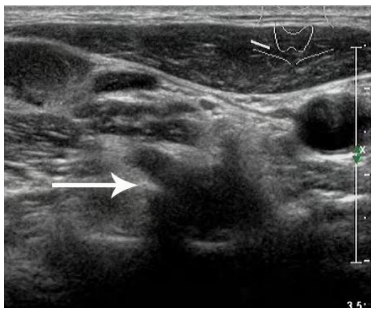

Figure 3 High-frequency color Doppler ultrasound image of the region where the brachial plexus root traverses the intervertebral foramen in healthy adults.

Nerve root shows an elliptic hypo-echo (arrow). Bony structure of transverse process of vertebra at the region where brachial plexus root traverses the intervertebral foramen is clearly displayed, with strong echo at the bilateral sides of the low-echo structure.

The region where the normal brachial plexus root traversed the intervertebral foramen exhibited a regular hypo-echo. The display rate of the C_{5-7} nerve root was 100%, and the display rates of C_8 and T_1 were, respectively, 83% (91/110) and 68% (75/110). Ultrasound clearly displayed no anterior tubercle or poorly developed anterior tubercle of the transverse process of the C_7 vertebra. Thus, the C_7 vertebra was used as a marker for localization of the nerve root.

Ultrasonic image characteristics of the brachial plexus at different observation planes

Intervertebral foramen plane: the lateral border of the sternocleidomastoid muscle was explored with a probe. The long axis of the brachial plexus displayed a striped echo texture at the region where the brachial plexus root traversed the intervertebral foramen. Ultrasonogram clearly revealed that the C_{5-7} nerve roots traversed the intervertebral foramen and projected outwards and downwards. The tilt angle of the C_5 nerve root was greater than that of the C_{6-7} nerve roots (Figure 4). Short axis images displayed a round or elliptic hypo-echo es structure (Figure 3).

Ultrasonic probe tracing on transverse sections outwards and downwards showed that the C_{5-7} nerve roots formed the upper and middle trunk of the brachial plexus. The deep cervical artery was frequently detected among the C_{7-8} nerve roots. The carotid artery and the internal jugular vein were distributed in the lateral part of the brachial plexus. Color Doppler ultrasound showed a pulsate flow signal. The T_1 nerve root could not be displayed due to obstruction by the clavicle and lung gas anterior to the nerve root. Because of their deep position, the display rates of the C_8 and T_1 nerve roots were, respectively, 83% (91/110) and 68% (75/110).

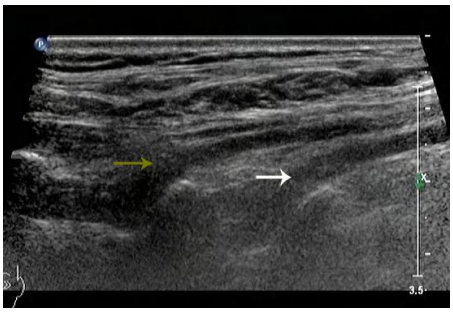

Figure 4 High-frequency color Doppler ultrasound image of brachial plexus on the intervertebral foramen plane in healthy adults.

C_{6-7} nerve roots traverse the intervertebral foramen and project outwards and downwards (arrows).

Interscalene plane: sweeping method used at the interscalene level (about C_6 level). The most superficial structure was the sternocleidomastoid muscle. Its cross section was triangular. Located near the deep surface of the sternocleidomastoid muscle were the anterior scalenus and medial scalenus muscles (located medially and laterally). The brachial plexus was located in the interscalene space, showing three hypo-echoes (Figure 5). There were significant differences in diameter, but no significant difference was detectable between the left and right sides (Table 2; $P > 0.05$). Its position was superficial, about 0.9 ± 0.2 cm under the skin. The cross-sectional areas of the short axial section of the upper, middle and lower trunks of the brachial plexus were, respectively, 0.07 cm^2, 0.09 cm^2 and 0.09 cm^2. In fact, the echo of the epineuria was similar to that of connective tissue, and was difficult to clearly discern.

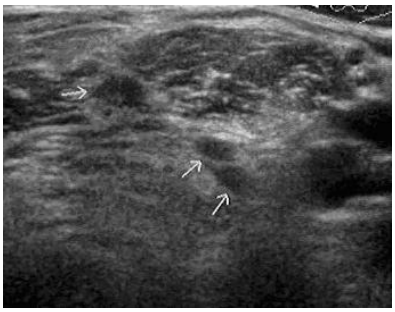

Figure 5 High-frequency color Doppler ultrasound image of the brachial plexus on the interscalene plane in healthy adults.

Brachial plexus distributed in interscalene, showing three hypo-echoes (arrows).

Table 2 Upper, middle, and lower trunks of the brachial plexus (mm) in the interscalene at left and right sides in healthy adults measured by high-frequency color Doppler ultrasonography

Side	Upper trunk	Middle trunk	Lower trunk
Left	2.18±0.38	2.46±0.32	2.74±0.33
Right	2.17±0.35	2.52±0.26	2.78±0.32

Data are expressed as mean ± SD, $n = 110$. Paired t-test showed no significant difference between the left and right sides for the upper, middle or lower trunks of the brachial plexus ($P > 0.05$).

Supraclavicular plane: coronal sections were made, and ultrasonograms exhibited the first rib, the pleural cupula and the subclavian artery. Ultrasound beam was vertical to the nerve trunk. Subclavian artery displayed pulsatile round hypo-echo. First rib presented curved linear strong echo, accompanied with sound shadow. Pleural cupula was located near the first rib. Brachial plexus was located anterolateral to the subclavian artery, showing round or elliptical low-echo structure. There were

significant differences in diameter and number. The distance between the nerve and skin was 0.9 ± 0.3 cm. The subclavian vein and anterior scalenus muscle were visible. Tubular and bunchy structures of the brachial plexus could be distinguished on the longitudinal plane. Botryoidal appearance was observed on the supraclavicular plane (Figure 6).

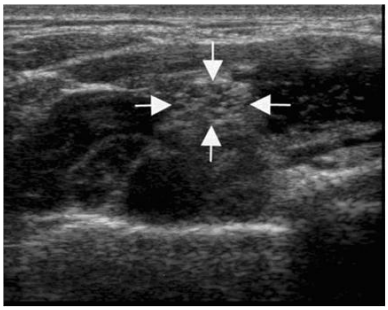

Figure 6 High-frequency color Doppler ultrasound image of the brachial plexus on the supraclavicular plane in healthy adults.

Arrows show a botryoidal appearance.

Infraclavicular plane: linear-array probe was placed 2 cm medial to the coracoid process. The nerve was localized to the deep surface of the pectoralis major and minor muscles. Three bunches of nerve trunk were found cephalic, lateral and posterior to the axillary artery, which presented a round hypo-echo, and the surrounding echo was enhanced (Figure 7). The distance between skin and nerve was 2.0 ± 0.6 cm. Brachial plexus was closest to the body surface above the infraclavicular plane to the back.

Figure 7 High-frequency color Doppler ultrasound image of the brachial plexus on the infraclavicular plane in healthy adults.

Three bunches of nerve trunk are found cephalic, lateral and posterior to the axillary artery, which exhibit a round hypo-echo (arrows).

Axillary brachial plexus plane: with the arm abducted, round or elliptic low-echo structure was visible posterior and lateral to the axillary artery and between the axillary artery and the axillary vein. Surrounding echo was slightly strong. The diameter was apparently smaller on the axillary brachial plexus plane compared with the above-described planes. Ultrasonogram in 67% (74/110) of subjects exhibited three nerve branches: median nerve, ulnar nerve and radial nerve (Figure 8). Five subjects had two branches. The distance between skin and nerve was 0.6 ± 0.3 cm. The nerve at this position exhibited great variability, and was mainly located at deep and superficial surfaces of the axillary artery, as well as at the anteroposterior position of the axillary artery.

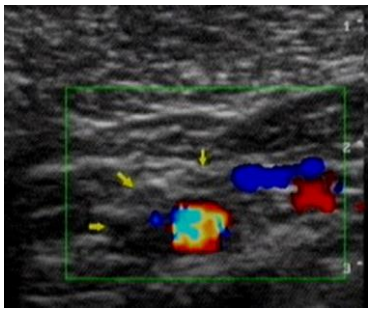

Figure 8 High-frequency color Doppler ultrasound image on the axillary brachial plexus plane in healthy adults.

Brachial plexus branches are located posterior and lateral to the axillary artery and between the axillary artery and the axillary vein, showing round or elliptic hypoechoic structure (arrows).

DISCUSSION

High-frequency ultrasound was utilized to observe the brachial plexus root. Compared with CT scanning, ultrasound clearly demonstrated that the anterior tubercle of the transverse process of the C_7 vertebra was small, even absent, which can be used to locate the C_7 vertebra. This is consistent with a previously published study[8]. The transverse process of the C_7 vertebra was long, and the posterior tubercle was obvious and large, but the anterior tubercle was absent or not developed. These anatomic characteristics can be used as a marker to identify the C_7 vertebral level. In the present study, we demonstrated that the nerve trunk of the brachial plexus on the longitudinal plane exhibited band-shaped echoes, with a regular boundary. High echoes were found at the edge, and the nerve exit zone was clear. Ultrasonogram on cross section presented round or elliptic low-echo structure, and the interior was composed of spot echoes surrounded by high echoes, which was not obvious due to the effects of the surrounding connective tissues. Ultrasonogram characteristics of the brachial plexus were presented histomorphologically. The nerve tract of hypo-echoes was surrounded by perineurium. The epineurium, with

high echoes, separated nerve clusters of hypo-echoes from other structures. The epineurium could be easily revealed in ultrasound, but the perineurium could be displayed in near-field using high-frequency probe scanning[6]. Therefore, linear high echoes appeared on the nerve cross section. Consequently, ultrasound exhibited band-shaped hypo-echo, and sometimes short-linear high echo appeared among the hypo-echo. In this study, the intervertebral foramen, the interscalene space, the supraclavicular and infraclavicular regions, and the axillary brachial plexus were observed using ultrasound. The morphology of the brachial plexus was different on different sections and using different probe directions. Peripheral nerve, ligament and tendon were visible on ultrasound. Color Doppler ultrasound can accurately identify arterial and venous vessels, and distinguish the nerve trunk. However, echoes of tendon, muscle and fascia sometimes overlapped that of the nerve trunk. When local muscle flexed and extended, tendon, muscle and fascia would change or move, but the position of the nerve trunk remained constant. Moreover, rotated movable probe scanning and suitable instrument parameters, such as penetration depth and gaining, can preferably identify round or elliptic low-echo structure of the nerve trunk on cross section and band-shaped echo on the longitudinal plane.

This study has confirmed that nerve root origin can be visible on ultrasound. C_{5-8} nerve roots traversed the intervertebral foramen and distributed outwards and downwards. During diagnosis of brachial plexus injury, we can precisely measure the diameter of the C_{5-7} nerve roots where they originate. In the present study, we concluded that the mean value of the diameter of the C_7 nerve roots was longest, which is consistent with the observation that the transverse diameter of the middle trunk is thicker than that of the upper trunk. Whether the transverse diameter of the lower trunk is thickest should be examined in a future investigation. Images of short-axis and long-axis sections of the C_{5-8} nerve roots at the nerve exit zone may be helpful to determine thinning of the diameter, echo drop-out, successive interruption or thickening of C_{5-8} nerve roots, meningocele and cyst formation, hemorrhage or cerebrospinal fluid leakage-induced encapsulated effusion, which would directly or indirectly diagnose brachial plexus injury and guide clinical therapy. Ultrasonometry of brachial plexus root and corresponding intervertebral foramen on the same level can be used to identify abnormities and provide imaging evidence of nerve-root-type cervical spondylosis, as well as increase the success rate of local anesthesia. Adjacent deep cervical artery can be used as a localization marker to diagnose C_{7-8} nerve root injury[9-11]. Ultrasonography of brachial plexus on interscalene plane displayed an interspace between the brachial plexus and the scalene muscle with a marrow top and wide bottom. The sternocleidomastoid muscle was superficially located. The anterior scalenus and medial scalenus muscles were deeply located. On about the sixth cervical vertebral level, we could distinguish the brachial plexus from other low-echo structures. The size of nerve was not consistent. There were frequently three nerves, including upper, middle and lower trunks. The distance among nerve trunks was different, sometimes short, sometimes long. This is the reason why anesthetic effects are poor in some local regions during brachial plexus anesthesia. The use of ultrasonic guidance of brachial plexus block could avoid poor anesthesia and reduce the dosage of anesthetics, which may result in optimal outcome using minimal dosage[12-13].

On the supraclavicular plane, the brachial plexus was parallel to the subclavian artery and located above the artery to the back. Thus, it is important to scan the cross section of subclavian artery on the midclavicular line. On the infraclavicular plane, the brachial plexus included three nerve tracts interior, lateral and posterior to the axillary artery. The position of the brachial plexus was deep at this position, so we should identify the brachial plexus by imaging the cross section of the axillary artery.

Based on the principle of ultrasonic imaging, we should measure the maximal diameter on the short-axis section where the nerve is perpendicular to the sound beam. We should not measure the diameter on longitudinal section. Deviation may occur, because of the position of the measurement point, or as a result of difference in level or declination of the sound beam[14]. Statistical analysis demonstrated no significant difference between left and right nerve trunks. The measurement values on the healthy side can be used as controls to judge normal or abnormal nerves.

In summary, a thorough understanding of the anatomical features of the brachial plexus using ultrasound is helpful to grasp the anatomical relationship between the brachial plexus root, trunk and tracts and the surrounding soft tissues, which permits an accurate description of the morphological feature of the brachial plexus intervertebral foramen and the nerve root. Anatomical localization of the brachial plexus can guide brachial plexus anesthesia, facilitate observation of the injured nerve after repair, and permit accurate localization.

SUBJECTS AND METHODS

Design

Neuroanatomical ultrasound imaging study.

Time and setting

Experiments were performed at the Shenzhen Second People's Hospital, China, from October 2008 to December 2011.

Subjects

110 healthy adults, who received body examination at the Medical Examination Center, Shenzhen Second People's Hospital, were included in this study. None of them experienced poor health conditions, or had shoulder or cervical malformation, trauma or history of surgery. There were 68 males and 42 females, averaging 32.5 (18–57) years old, weighing 45–90 kg. They underwent ultrasound scanning. A total of 20 volunteers, comprising 12 males and 8 females, averaging 31.5 (23–46) years old, weighing 45–80 kg, were randomly selected to receive cervical CT scanning. All subjects were informed of study content and signed informed consent. The study was conducted in accordance with the ethical requirements of the *Declaration of Helsinki*.

Methods

Ultrasound scanning

IU22 type (Philips, Bothell, WA, USA) and Mylab30 type (Esaote, Florence, Italia) color Doppler ultrasonographs were utilized, with linear probes at 5– 12 MHz frequency. The subjects lied at a supine position. Nerve root was scanned on cervical cross section when subject's head was in the middle position, with the probe gliding up and down. Cervical interscalene and supraclavicular plane were scanned with the subject's head turned to the contralateral side and the arm abducted. The angle between the arm and the body was about 60°. Using the direct contact method, the probe was vertical to the skin, gliding up and down. When the infraclavicular plane was scanned, the subject's head was in the middle position, with the arm laid naturally. Axillary scanning was conducted when the subject's head was in the middle position with the arm abducted at an angle of 90°. The forelimb was in a "salute" posture. Color Doppler and pulse Doppler ultrasounds were employed to judge adjacent great blood vessels and to identify the relationship of muscle, artery and vein to the brachial plexus at various regions, and to observe the morphology and distribution of the nerve. Intervertebral foramen, interscalene, supraclavicular, infraclavicular and the axillary brachial plexus were observed in relation to the anatomic features, and a comparison was done between left and right sides. The diameter of interscalene brachial plexus and the distance from the body surface were recorded.

CT scanning

CT scanning was done using a Sensation 4 spiral CT scanner (Siemens, Henkestrasse, Erlangen, Germany), at tube tension of 20 kV, tube current of 60 mAs, and slice thickness of 6 mm.

Statistical analysis

The data were analyzed using SPSS 13.0 software (SPSS, Chicago, IL, USA). Measurement data were expressed as mean ± SD. A comparison between left and right sides was done using paired *t*-test. One-way analysis of variance was used among different methods. A value of $P < 0.05$ was considered statistically significant.

Acknowledgments: We thank Professor Guozhao Teng from the Department of Statistics, Shenzhen Second People's Hospital in China for the support of statistical analysis, and associate professor Xixiong Qiu from the Department of Radiology for the support of CT examination.

Funding: This project was funded by the Fundamental Research Funds for the Higher Learning Schools of Youth Teacher Education Program of Sun Yat-sen University in 2009, No. 09YKPY05; and the Natural Science Foundation of Guangdong Province, No. S2011010004708.

Author contributions: Zhengyi Li participated in study concept, design, data collection, integration and analysis, and manuscript writing. Xun Xia and Xiaoming Rong were in charge of statistical analysis and provided technical support. Yamei Tang obtained the funding. Dachuan Xu and Yamei Tang provided technical and data support and served as principle investigators.

Conflicts of interest: None declared.

Ethical approval: This study was approved by the Ethics Committee, Shenzhen Second People's Hospital in China.

REFERENCES

[1] De Tran QH, Clemente A, Doan J, et al. Brachial plexus blocks: a review of approaches and techniques. Can J Anaesth. 2007;54(8):662-674.

[2] Lahori VU, Raina A, Gulati S. A randomized comparative study of efficacy of axillary and infraclavicular approaches for brachial plexus block for upper limb surgery using peripheral nerve stimulator. Indian J Anaesth. 2011;55(3): 253-259.

[3] Christ S, Rindfleisch F, Friederich P. Superficial cervical plexus neuropathy after single-injection interscalene brachial plexus block. Anesth Analg. 2009;109(6): 2008-2011.
[4] Jin LL, Xu XZ, Wu DZ, et al. Ultrasonographic investigation of the brachial plexus. Zhonghua Shouwaike Zazhi. 2007;23(4):248-251.
[5] Chen DZ, Cong R, Zheng MJ, et al. Differential diagnosis between pre-and postganglionic adult traumatic brachial plexus lesions by ultrasonography. Ultrasound Med Biol. 2011;37(8):1196-1203.
[6] Kubiena H, Hormann M, Michlits W, et al. Intraoperative imaging of the brachial plexus by high-resolution ultrasound. J Reconstr Microsurg. 2005;21(7):429-433.
[7] Royse CE, Sha S, Soeding PF, et al. Anatomical study of the branchial plexus using surface ultrasound. Anaesth Intensive Care. 2006;34(2):203-210.
[8] Martinoli C, Bianchi S, Santacroce E, et al. Brachial plexus sonography: a technique for assessing the root level. AJR Am J Roentgenol. 2002;179(3):699-702.
[9] Graif M, Martinoli C, Rochkind S, et al. Sonographic evaluation of brachial plexus pathology. Eur Radiol. 2004;14(2):193-200.
[10] Shafighi M, Gurunluoglu R, Ninkovic M, et al. Ultrasonography for depiction of branchial plexus injury. J Ultrasound Med. 2003;22(6):631-634.
[11] Dolan J, Williams A, Murney E, et al. Ultrasound guided fascia iliaca block: a comparison with the loss of resistance technique. Reg Anesth Pain Med. 2008; 33(6):526-531.
[12] Bowens CJ, Briggs ER, Malchow RJ, et al. Brachial plexus entrapment of interscalene nerve catheter after uncomplicated ultrasound-guided placement. Pain Med. 2011;12(7):1117-1120.
[13] Harper GK, Stafford MA, Hill DA, et al. Minimum volume of local anaesthetic required to surround each of the constituent nerves of the axillary brachial plexus, using ultrasound guidance: a pilot study. Br J Anaesth. 2010; 104(5):633-636.
[14] Zaidman CM, Al-Lozi M, Pestronk A. Peripheral nerve size in normals and patients with polyneuropathy: an ultrasound study. Muscle Nerve. 2009;40(6):960-966.

(Edited by Li RX, Wang JL/Qiu Y/Song LP)